AIP Applied Physics Letters

Role of joule heating effect and bulk-surface phases in voltage-driven metal-insulator transition in VO2 crystal

Bongjin Simon Mun, Joonseok Yoon, Sung-Kwan Mo, Kai Chen, Nobumichi Tamura, Catherine Dejoie, Martin Kunz, Zhi Liu, Changwoo Park, Kyungsun Moon, and Honglyoul Ju

Citation: Applied Physics Letters **103**, 061902 (2013); doi: 10.1063/1.4817727
View online: http://dx.doi.org/10.1063/1.4817727
View Table of Contents: http://scitation.aip.org/content/aip/journal/apl/103/6?ver=pdfcov
Published by the AIP Publishing

Articles you may be interested in
Comprehensive study of the metal-insulator transition in pulsed laser deposited epitaxial VO2 thin films
J. Appl. Phys. **113**, 043707 (2013); 10.1063/1.4788804

Heteroepitaxial VO2 thin films on GaN: Structure and metal-insulator transition characteristics
J. Appl. Phys. **112**, 074114 (2012); 10.1063/1.4758185

Electrically-driven metal-insulator transition with tunable threshold voltage in a VO2-SmNiO3 heterostructure on silicon
J. Appl. Phys. **110**, 026110 (2011); 10.1063/1.3610798

Geometric confinement effects on the metal-insulator transition temperature and stress relaxation in VO2 thin films grown on silicon
J. Appl. Phys. **109**, 063512 (2011); 10.1063/1.3556756

The metal-insulator transition in vanadium dioxide: A view at bulk and surface contributions for thin films and the effect of annealing
J. Appl. Phys. **105**, 114322 (2009); 10.1063/1.3143787


Not all AFMs are created equal
Asylum Research Cypher™ AFMs
There's no other AFM like Cypher
www.AsylumResearch.com/NoOtherAFMLikeIt
OXFORD INSTRUMENTS
The Business of Science®

This article is copyrighted as indicated in the article. Reuse of AIP content is subject to the terms at: http://scitation.aip.org/termsconditions. Downloaded to IP: 117.32.153.170 On: Tue, 04 Nov 2014 03:06:36

APPLIED PHYSICS LETTERS **103**, 061902 (2013)

Role of joule heating effect and bulk-surface phases in voltage-driven metal-insulator transition in VO_2 crystal

Bongjin Simon Mun,[1,a)] Joonseok Yoon,[2] Sung-Kwan Mo,[3] Kai Chen,[3,4] Nobumichi Tamura,[3] Catherine Dejoie,[3] Martin Kunz,[3] Zhi Liu,[3] Changwoo Park,[5] Kyungsun Moon,[2] and Honglyoul Ju[2,a)]

[1]*Department of Physics and Photon Science, School of Physics and Chemistry, Ertl Center for Electrochemistry and Catalyst, Gwangju Institute of Science and Technology, Gwangju 500-712, South Korea*
[2]*Department of Physics, Yonsei University, Seoul 120-749, South Korea*
[3]*Advanced Light Source, Lawrence Berkeley National Laboratory, Berkeley, California 94720, USA*
[4]*Center for Advancing Materials Performance from the Nanoscale (CAMP-Nano), State Key Laboratory for Mechanical Behavior of Materials, Xi'an Jiaotong University, Xi'an 710049, China*
[5]*Division of Applied Chemistry and Biotechnology, Hanbat National University, Daejon 305-719, South Korea and Advanced Nano Products, Chungwon, Chungbuk 363-942, South Korea*

(Received 10 April 2013; accepted 21 July 2013; published online 6 August 2013)

We report the characteristics of a voltage-induced metal-insulator transition (MIT) in macro-sized VO_2 crystals. The square of MIT onset voltage ($V_{CMIT}{}^2$) value shows a linear dependence with the ambient temperature, suggesting that the Joule heating effect is the likely cause to the voltage-induced MIT. The combination of optical microscope images and Laue microdiffraction patterns show the simultaneous presence of a metallic phase in the bulk of the crystal with partially insulating surface layers even after the MIT occurs. A large asymmetry in the heating power just before and after the MIT reflects the sudden exchange of Joule heat to its environment. © *2013 Author(s). All article content, except where otherwise noted, is licensed under a Creative Commons Attribution 3.0 Unported License.* [http://dx.doi.org/10.1063/1.4817727]

Strongly correlated materials (SCMs) exhibit many remarkable physical properties, such as metal-insulator transition (MIT), high temperature superconductivity, and colossal magnetoresistance. Complex interplays between electrons, phonons, and spin are known to be at the root of these unique properties.[1] Among SCMs, VO_2 is a unique material in that its MIT occurs near room temperature (~67 °C) and is accompanied by a structural phase transition (SPT), from an insulating monoclinic (M1) phase to a metallic rutile (R) phase.[2] The MIT in VO_2 can be either due to strong electron-electron interaction, or strong electron-lattice interaction, or a combination of the two.[2–9] However, the coexistence of these interactions makes it difficult to identify the primary cause of the MIT. From the view of the practical application of the MIT characteristics of VO_2 in electrical/optical devices, it is essential to understand the intrinsic driving force of the voltage-induced MIT. Kim *et al.*[10] have reported that the voltage-induced MIT in VO_2 films occurs without SPT, when the external field is large enough to induce the carrier density to be above a critical carrier density (n_c) of $\sim 3 \times 10^{18}\,\mathrm{cm}^{-3}$, supporting a field-induced breakdown mechanism. On the other hand, numerous alternate reports do not support this model.[11,12] In the report of Kim *et al.*, the magnitudes of the critical electric field (E_C) at the MIT appeared to be less than 1 V/μm, a value much smaller than the theoretical estimated value of $E_C = 50\,\mathrm{V}/\mu\mathrm{m}$. This theoretical value of E_C has been calculated from the electric field required for inducing the critical concentration of carriers ($\sim 3 \times 10^{18}\,\mathrm{cm}^{-3}$) in VO_2 by the field-induced Poole–Frenkel effect.[13] In fact, there are large variations in experimental E_C values reported in the literature, varying from ~0.05 to ~20 V/μm.

In this letter, we report on the characteristics of the voltage-induced MIT in macro-sized VO_2 single crystals. Various experimental tools, such as transport measurements, optical microscopy, and synchrotron-based x-ray microdiffraction, were applied to investigate the MIT properties. Our results suggest that the voltage-induced MIT in VO_2 crystals occurs via a Joule heating effect rather than a field-induced breakdown effect. Also, the voltage-induced metallic state of VO_2 crystals is composed of the metallic phase in the bulk of the crystal with partially insulating surface layers, indicating different MIT behaviors at the surface.

VO_2 single crystals were synthesized with a self-flux method, the details of which are reported elsewhere.[9] The crystals have an average length of 1–3 mm and width of 0.05–0.10 mm with a square cross section. No other chemical elements were found except for vanadium and oxygen from energy dispersive X-ray spectroscopy (EDS) measurements. Temperature vs resistance (*T-R*) and voltage vs current (*V-I*) measurements of VO_2 crystals were performed using a dc two-contact four-probe method. During *V-I* measurements, the crystals were connected in series with either a 10 kΩ or a 6.4 kΩ resistor (R_{EXT}) as shunt resistance to protect the crystal and instruments. Optical microscopy was employed to monitor the metallic and insulating phases of VO_2 during the temperature-driven and voltage-induced MIT measurements. To investigate the SPT during the voltage-induced MIT, synchrotron-based x-ray Laue microdiffraction (μ-XRD) was carried out on Beamline 12.3.2 at the Advanced Light Source at Lawrence Berkeley National Laboratory.[14]

[a)] Authors to whom correspondence should be addressed. Electronic addresses: bsmun@gist.ac.kr and tesl@yonsei.ac.kr

0003-6951/2013/103(6)/061902/5

Fig. 1(a) shows a series of *V-I* curves measured as the applied bias voltage is increased at different temperatures (T_A) in the range of 40 to 65 °C. The inset picture illustrates the schematics of the circuit constructed for the *V-I* measurements with the VO_2 crystal sample, in which the current was measured as the voltage was increased. The resistance of external resistor was measured independently and applied for the observed values. When the external voltage was ramped up starting from zero, the current increased linearly with the initial slopes corresponding to resistances of $(4.0 \sim 10.0) \times 10^4\ \Omega$ for each temperature. When the voltage reached the MIT onset value (V_{MIT}), the current suddenly jumped to a value 5 to 6 times higher than the one before the MIT. Just before the MIT, the sample resistance is almost independent of the temperature with values in the range of $(2.2–3.0) \times 10^4\ \Omega$. Just before the MIT, the resistance (R_{CMIT-}) of the crystal is a few times larger than R_{EXT}. However, immediately after the MIT, the resistance of the crystal, estimated to be less than $\sim 10\ \Omega$, drops to a value much smaller than R_{EXT} ($6.4 \times 10^3\ \Omega$). Consequently, the entire load from the external voltage is applied to the external resistor after the MIT. Since the magnitude of the current after the MIT is determined by R_{EXT}, the current jump ratio $(\frac{I_{MIT+}}{I_{MIT-}})$ is equal to $\frac{R_{CMIT-}}{R_{EXT}} + 1$, where $I_{MIT+} = \frac{V_{MIT}}{R_{CMIT-}+R_{EXT}}$ and $I_{MIT\_} = \frac{V_{MIT}}{R_{EXT}}$ are the current just after and just before MIT, respectively. Thus, the ratio of R_{CMIT}/R_{EXT} determines the current jump ratio. As expected, V_{MIT} monotonically decreases with increasing ambient temperature from 27.5 V at 40 °C to 8.6 V at 65 °C. Before the MIT, the applied external voltage is shared between the crystal and the resistor. In this case, the voltage (V_{CMIT}) across the crystal can be obtained as $\frac{V_{MIT}R_{CMIT-}}{R_{CMIT-}+R_{EXT}}$, with values of 22.5, 16.7, 12.9, 10.7, and 6.8 V at 40, 50, 55, 60, and 65 °C, respectively. The magnitude of the critical electric field (E_{CMIT}) at the MIT, defined as V_{CMIT}/L (L: the crystal length) is linked to the origin of the voltage-induced MIT and our E_C values vary from 3.0×10^{-2} V/μm at $T_A = 65$ °C to 0.11 V/μm at $T_A = 40$ °C. Interestingly, the magnitude of the critical field is less than 0.25% of the theoretical estimate of 50 V/μm, to generate a carrier concentration of $\sim 3 \times 10^{18}\ \mathrm{cm}^{-3}$ inside VO_2 in the field-induced breakdown model.[15] It is possible that the presence of defects can lower the critical fields. However, the defect density in high quality VO_2 crystal is expected to be much smaller than the one in VO_2 thin films. Considering this significant difference in magnitude of the critical field, it appears to be very difficult to explain the origin of the voltage-induced MIT in the framework of the field-induced breakdown model.

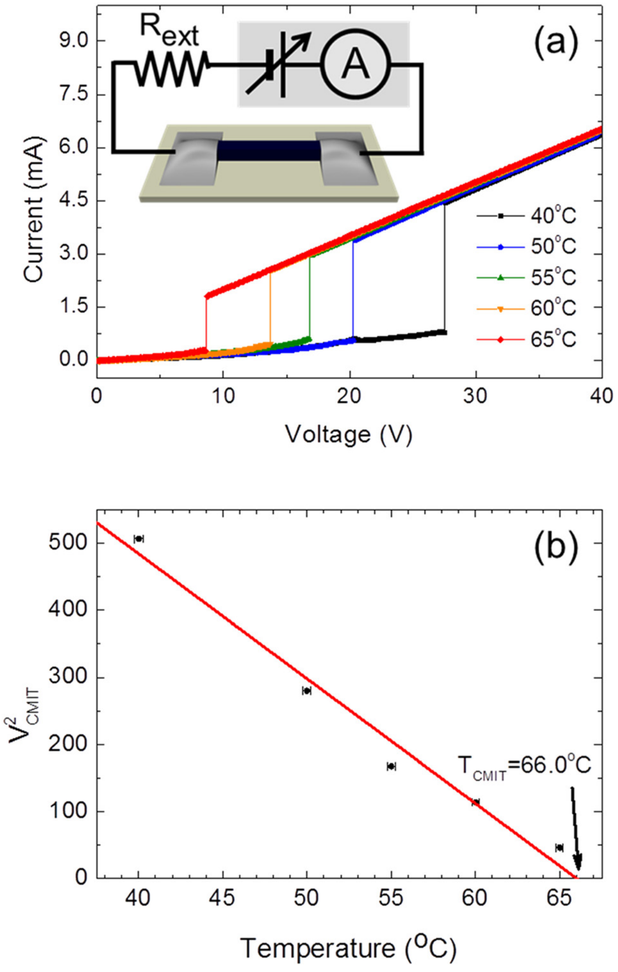

FIG. 1. (a) *V-I* curves measured by increasing the applied bias voltage at varying temperatures (T_A) in the range between 40–65 °C. The inset shows a schematic drawing of the sample geometry used to carry out the voltage induced transitions. (b) A plot of $V_{CMIT}{}^2$ versus T_A, where V_{CMIT} is the voltage on the crystal just before MIT.

As an alternative model to explain the voltage-induced MIT, we have tested the Joule heating model. First, we tested whether the temperature dependence of the critical voltage agrees with predictions from Joule heating. In this model, the MIT occurs when the voltage-induced Joule heating is sufficient to raise the crystal temperature to the MIT temperature (~67 °C). Assuming the heat obtained in the VO_2 crystal is mainly due to the balance between resistive Joule heat and heat loss from the crystal to the environment via heat conduction, this relation can be expressed by the following simple heat equation:

$$\frac{dQ}{dt} = \frac{V_C^2}{R_C} - k(T_C - T_A), \tag{1}$$

where Q, V_C, k, and T_C are the total net heat in the crystal, the voltage drop across the crystal, the effective thermal conductance, and the crystal temperature, respectively. Since the resistance between the contact and the VO_2 sample is low compared to the resistance of the crystal, when VO_2 is in the insulating state, the contact resistance is ignored in our treatment. When the generated heat due to Joule heating is equal to the heat loss via thermal conduction to the surroundings, a steady state condition ($\frac{dQ}{dt} = 0$) is reached. At this steady state, the crystal temperature T_C is equal to $T_A + \frac{V_C^2}{kR_C}$ and can be further increased as bias voltage increases. Finally, the crystal temperature of the critical MIT temperature, T_{CMIT}, can be reached when sufficient bias voltage is applied. Thus, V_{CMIT} can be expressed as

$$V_{CMIT}{}^2 = kR_{CMIT\_}(T_{CMIT}\text{-}T_A). \tag{2}$$

In Fig. 1(b), $V_{CMIT}{}^2$ versus T_A is plotted. The linearity of the fitted curve in Fig. 1(b) confirms that a Joule heating model

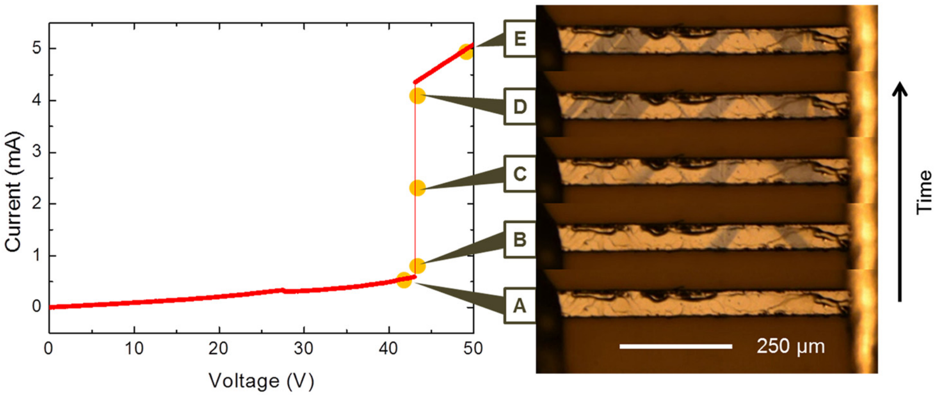

FIG. 2. (Left) Voltage (V) versus current (I) curves and (Right) optical microscopy images as a function of increasing voltage at temperature (T_A) of 40.0 °C.

is appropriate to explain the voltage-induced transition of the crystal. Extrapolation of the fitted line to the temperature axis gives the T_{CMIT}. Least-square fitting provides the values of T_{CMIT} and kR_{CMIT-} as 66.0 (±1.1) °C and 18.6 $V^2/°C$, respectively. The experimentally determined T_{CMIT} is in good agreement with the known MIT temperature of 67 °C. Using the value of $R_{CMIT-} = (2.2 \sim 3.0) \times 10^4\,\Omega$, estimated from the V-I curve in Fig. 1, we found the effective thermal conductance k to be $(6.4 \sim 8.6) \times 10^{-4}$ W/°C.

Considering the fact that these metallic and insulating phases of VO_2 generate a significant contrast in optical reflectivity, monitoring the presence, and its motion of the phase boundary during the voltage induced MIT is possible by using optical microscopy.[8] The dark and bright areas in the optical microscope pictures represent the metallic and insulating states of VO_2, respectively. Figure 2 displays both the V-I curve (left hand side of Fig. 2) and optical microscopy images (right hand side of Fig. 2) recorded simultaneously as a function of increasing voltage at T_A of 40.0 °C. Optical microscope images in Fig. 2 show the formation of multiple phase boundaries as a function of time during the voltage-induced MIT (voltage ramp rate = 0.2 V/s). The time interval covered is about 0.5 s and images are therefore ~0.1 s apart. The sizes of the metallic and insulating phases are of macroscopic scale, in contrast to the metallic nano-puddles observed in thin films.[5] The optical image A in Fig. 2 represents the insulating phases of VO_2, corresponding to a small flow of current and only the insulating phase is visible on the surface. However, in images B ~ D at the onset of the MIT, the surface shows the presence of both insulating (bright) and metallic (dark) phases. Interestingly, a combination of metallic and insulating phases remains at the surface even after $V > V_{MIT}$. The optical image E of Fig. 2 taken at $V > V_{MIT}$ shows the metallic phase occupying an area of 39% and the insulating phase occupying an area of 61%. However, from the V-I curve for $V > V_{MIT}$, the crystal resistance was measured to be less than 0.2% of R_{EXT}, which clearly suggests that the entire crystal should be in its metallic state. Since the optical microscope images reflect the surface properties of the crystal, the likely explanation for this discrepancy is that the bulk of the crystal is in conducting state, while some portions of the surface remain in the insulating state. This possibility was tested by applying bulk sensitive x-ray microdiffraction experiments. The probing depth of Laue diffraction is much larger than the crystal thickness,[16] while the optical microscope images reflect the surface sensitive properties of the crystal.

Figure 3 shows both the V-I curve and the Laue diffraction patterns which were recorded simultaneously as a function of increasing voltage at $T_A = 40$ °C, a temperature identical to the one used in the optical microscope measurement in Fig. 2. In the Laue diffraction experiment, a single line scan of Laue patterns was collected with a step size of 2 μm after the external voltage was set, while the V-I curve was measured in parallel. The time interval between different

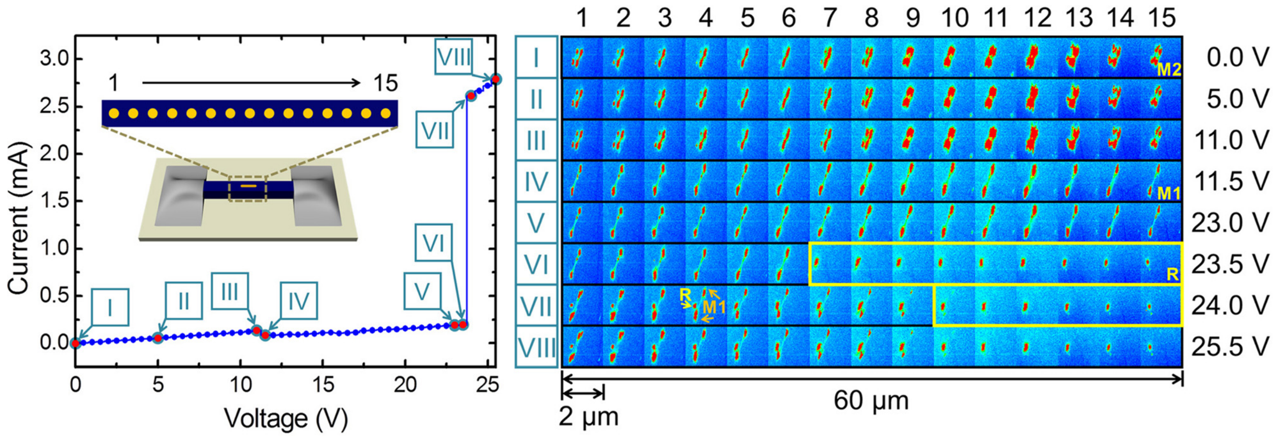

FIG. 3. (Left) Schematic of x-ray microdiffraction experiment setup and (Right) the voltage (V) versus current (I) curves measured during the x-ray diffraction measurement simultaneously. The M1, M2, and R represent insulating monoclinic phase 1, insulating monoclinic phase 2, and metallic rutile phase, respectively.

voltage sets is 180 s. For easy comparison, only 15 out of a total of 30 diffraction images are shown at the critical voltage set points. Literature values of the lattice parameters were used to index the Laue diffraction patterns[7] and its structures are marked on the Laue diffraction patterns in Fig. 3. The diffraction images of Fig. 3 show that our VO_2 sample is in a pure monoclinic insulating M2 phase at 0.0 V voltage (I). The M2 phase remained up to 11.0 V (III). However, this M2 phase suddenly changes to the M1 phase as the voltage is increased above 11.0 V (III to IV). Simultaneously, the *V-I* curve shows a small kink near 11.0 V, which was also shown at ∼27.0 V in Fig. 2. It indicates that Joule heating at this voltage is sufficient enough to raise the crystal temperature for the M2-M1 insulating-insulating phase transition (IIT). This IIT was previously reported for VO_2 single crystals[8,9] and different IIT set voltages were found for different sample sizes, indicating a size effect. The different IIT voltage values of Figs. 2 and 3 are due to the different sample sizes. Above 11.5 V, only the pure monoclinic insulating M1 phase was observed, and this M1 phase remained stable up to V_{MIT}. When the voltage reached 23.5 V (VI), individual diffraction images along the scan line show variably either the tetragonal metallic R (images #7 ∼ 15) or the insulating M1 phases (images #1 ∼ 6), yet the *V-I* curve indicates the sample to be in the insulating state at this voltage. Finally, when the voltage reached V_{MIT}, 24.0 V (VII), the metallic R phase starts to appear together with the M1 phase on the left hand side (#1 ∼ 9), while only the R phases remain on the right hand side of sample (#10 ∼ 15). At the voltage above V_{MIT} (VIII), diffraction patterns remain identical to the one from 24.0 V. That is, the insulating M1 phase still exists together with metallic R phase even after the sample is in full metallic states. As mentioned above, there is a big difference in bulk sensitivity from Laue diffraction to optical microscope. Therefore, the coexistence of M1 and R phases on the left hand side of Fig. 3 at $V > V_{MIT}$ confirms the finding from optical microscopy (Fig. 2), i.e., that half of VO_2 crystals are composed of the metallic phase in the body of the crystal with a partially insulating surface skin layer. The conducting path for the electrons is dominated by the bulk. One thing to note is that there is a shift of the phase boundary from 23.5 V to 24.0 V, outlined with yellow in Fig. 3. In fact, this shift of the phase boundary during the MIT reveals evidence for local thermal fluctuations between surface skin layer and bulk layer, as discussed below.

First, it is important to understand how this insulating surface skin layer is formed as this will provide critical insights on the origin of the voltage-induced MIT in VO_2. Immediately after the MIT, the entire applied voltage goes into the external series resistor since the resistance in the VO_2 metallic phase is negligible compared to R_{EXT}. The heating power (I^2R_C) just before and just after the MIT is estimated to be $I_{MIT-}{}^2R_{CMIT-} \sim 2.2 \times 10^{-2}$ W and $I_{MIT+}{}^2R_{CMIT+} \sim$ less than 3.8×10^{-4} W, respectively. As can be seen, the heating power just after the MIT is much reduced compared to just before MIT. (R_{CMIT+} is the crystal resistance just after the MIT.) Therefore, immediately after the MIT ($V > V_{MIT}$) the temperature of the sample cannot be further increased because of the significant drop of heating power due to the low resistance in the sample. This large asymmetry in the heating power around the MIT can be viewed as an on-off heating power switch, i.e., the switch is on before the MIT and off after the MIT; this keeps the crystal at the MIT temperature. Our result is also consistent with a recent report made by Zimmers *et al.*, in which the presence of the thermal heating effect on the voltage-induced MIT in VO_2 is observed by fluorescence spectroscopy.[17] Also, it will be important to understand this insulating skin layer in the future applications of VO_2 in memory devices.

The sudden change of heating power at the MIT can be also applied to explain the shift of the observed phase boundary in Fig. 3. At the onset of MIT, 23.5 V (VI) in Fig. 3, the metallic R phase starts to propagate from the right to the left and more than half of the sample area is covered with the metallic phase (#7 ∼ 15 in VI). Once the sample reached the full conducting state at 24.0 V (VII), the heating power is lost cooling the sample from the surface and the insulating skin layer is formed (#7 ∼ 9 in VII), as shown in Fig. 3. The origin of these mixed states, R and M1 phases, is not clearly known at the moment. There could be local fluctuations of sample thickness which could generate different heat losses during the voltage-driven MIT. In turn, the sample can form localized insulating skin layer. Considering that the temperature-driven MIT does not show the mixed state in previous reports,[8,9] it is likely that the mechanism of the Joule heating effect in the voltage-driven MIT causes results of Figs. 2 and 3. When the substrate temperature is raised to 67 °C, which is near to the critical temperature of the temperature-driven MIT, no mixed states are observed from optical microscope images.

Our results show that the voltage-induced MIT in a macroscopic VO_2 crystal occurs due to the Joule heating effect under the conditions of the present experiment. A self-switching effect, which is caused by the large asymmetry in heating power just before and after the MIT, allows to maintain the crystal temperature at MIT temperature.

H. L. Ju and B. S. Mun would like to thank the support by Basic Science Research Program through the National Research Foundation of Korea (NRF) funded by the Ministry of Education, Science and Technology (2012R1A1A2006948 and 2012R1A1A2001745). The Advanced Light Source is supported by the Director, Office of Science, Office of Basic Energy Sciences, Materials Science Division, of the US Department of Energy under Contract No. DE-AC02-05CH11231 at LBNL. The microdiffraction program at the ALS on BL 12.3.2 was made possible by NSF Grant No. 0416243. This paper was supported by GIST College's 2013 GUP Research Fund.

[1] M. Imada, A. Fujimori, and Y. Tokura, Rev. Mod. Phys. **70**, 1039 (1998).

[2] J. Morin, Phys. Rev. Lett. **3**, 34 (1959).

[3] N. F. Mott, Rev. Mod. Phys. **40**, 677 (1968).

[4] A. Zylbersztejn and N. F. Mott, Phys. Rev. B **11**, 4383 (1975).

[5] M. M. Qazilbash, M. Brehm, B. G. Chae, P. C. Ho, G. O. Andreev, B. J. Kim, S. J. Yun, A. V. Balatsky, M. B. Maple, F. Keilmann, H. T. Kim, and D. N. Basov, Science **318**, 1750 (2007).

[6] H. T. Kim, Y. W. Lee, B. J. Kim, B. G. Chae, S. J. Yun, K. Y. Kang, K. J. Han, K. J. Yee, and Y. S. Lim, Phys. Rev. Lett. **97**, 266401 (2006).

[7] J. Cao, Y. Gu, W. Fan, L. Q. Chen, D. F. Ogletree, K. Chen, N. Tamura, M. Kunz, C. Barrett, J. Seidel, and J. Wu, Nano Lett. **10**, 2667 (2010).

[8] B. S. Mun, K. Chen, J. Yoon, C. Dejoie, N. Tamura, M. Kunz, Z. Liu, M. E. Grass, S.-K. Mo, C. Park, Y. Y. Lee, and H. Ju, Phys. Rev. B **84**, 113109 (2011).

[9] B. S. Mun, K. Chen, Y. Leem, C. Dejoie, N. Tamura, M. Kunz, Z. Liu, M. E. Grass, C. Park, J. Yoon, Y. Y. Lee, and H. Ju, Phys. Status Solidi (RRL) **5**, 107 (2011).

[10] B. J. Kim, Y. W. Lee, S. Choi, J. W. Lim, S. J. Yun, H. T. Kim, T. J. Shin, and H. S. Yun, Phys. Rev. B **77**, 235401 (2008).

[11] J. M. Baik, M. H. Kim, C. Larson, A. M. Wodtke, and M. Moskovits, J. Phys. Chem. C **112**, 13328 (2008).

[12] X. Zhong, X. Zhang, A. Gupta, and P. LeClair, J. Appl. Phys. **110**, 084516 (2011).

[13] S. Hormoz and S. Ramanathan, Solid-State Electron. **54**, 654 (2010).

[14] M. Kunz, N. Tamura, K. Chen, A. A. MacDowell, R. S. Celestre, M. M. Church, S. Fakra, E. E. Domning, J. M. Glossinger, J. L. Kirschman, G. Y. Morrison, D. W. Plate, B. V. Smith, T. Warwick, V. V. Yashchuk, H. A. Padmore, and E. Ustundag, Rev. Sci. Instrum. **80**, 035108 (2009).

[15] H.-T. Kim, B.-G. Chae, D.-H. Youn, S.-L. Maeng, G. Kim, K.-Y. Kang, and Y.-S. Lim, New J. Phys. **6**, 52 (2004).

[16] B. L. Henke, E. M. Gullikson, and J. C. Davis, At. Data Nucl. Data Tables **54**(2), 181–342 (1993).

[17] A. Zimmers, L. Aigouy, M. Mortier, A. Sharoni, S. Wang, K. G. West, J. G. Ramirez, and I. K. Schuller, Phys. Rev. Lett. **110**, 056601 (2013).